# Penetration by Shaped Charge Jets of Nonuniform Velocity

G. R. Abrahamson and J. N. Goodier

Citation: Journal of Applied Physics **34**, 195 (1963); doi: 10.1063/1.1729065
View online: http://dx.doi.org/10.1063/1.1729065
View Table of Contents: http://scitation.aip.org/content/aip/journal/jap/34/1?ver=pdfcov
Published by the AIP Publishing



# Penetration by Shaped Charge Jets of Nonuniform Velocity*

G. R. ABRAHAMSON† AND J. N. GOODIER‡
*Stanford Research Institute, Menlo Park, California*
(Received 12 July 1962)

The simple hydrodynamic theory of penetration by shaped charge jets is extended to include nonuniform jet velocity distributions and stand-off distance. The penetration of a jet with an initial linear velocity distribution is compared to an ideal upper limit and is found to be close to the maximum obtainable in practice. The conclusions concern idealized jets, without regard to the performance limitations which break-up and waver impose on real jets.

## I. INTRODUCTION

THE development of a high velocity jet from a conical metal shell which is projected toward the axis by an explosive charge is illustrated by Fig. 1. Such jets, commonly call shaped charge jets, are easily able to penetrate several cone diameters into metal or rock targets and hence have many important applications.

Figure 2 shows a jet emerging from a shaped charge. The decrease in the diameter of the jet as it travels is due to stretching caused by the velocity gradient along the jet. As indicated elsewhere,[1,2] formation of the jet and subsequent penetration of a target are essentially independent processes. Thus, they may be considered separately; this greatly simplifies the analysis.

The basic theory of penetration by shaped charge jets was given over a decade ago.[1,2] Using simple concepts of ideal incompressible hydrodynamics, it was shown that the penetration of a continuous jet of uniform velocity should be proportional to the length of the jet and the square root of the ratio of jet density to target density. Eichelberger,[3] Singh,[4] and Cook[5] showed that the simple hydrodynamic theory is valid for jet velocities greater than 0.4 cm/$\mu$sec. At lower velocities the strength of the jet and target become important and actual penetration is less than predicted.[3,4–6] Modifications of the simple theory have been advanced to account for jet and target strength at low jet velocities.[3–5]

With typical shaped charges, jet velocity decreases monotonically from front to rear. Thus the jet stretches as it travels toward the target and arrives with increased length, thereby giving greater penetration than a jet of uniform velocity. As the distance from charge to target (stand-off distance) is increased, stretching due to nonuniform jet velocity is enhanced. However, deviations from perfect axial alignment (waver) and break-up[7] of the jet from excessive stretching (see Figs. 3 and 4) cause penetration to decrease at stand-off distances greater than a few cone diameters. The original investigators[1,2] recognized the effects of nonuniform jet velocity and stand-off on penetration and treated them qualitatively. In the present paper the simple hydrodynamic theory is extended to include these effects. Since waver and break-up are not included, it is an investigation of what could be attained, or approached, if these effects could be eliminated. As in the original theory, the basic idealization is that the jet and target behave as ideal incompressible fluids at the extremely high pressures generated by impact of the jet.

## II. THEORY

Figure 5 shows a jet approaching a target. The jet at this instant, $t=0$, is of length $l$ and has a velocity distribution $v(x)$. Taking $\xi$ as the initial $x$ coordinate of the element which will arrive at the target (bottom of the hole) at time $t$, and assuming that the velocity $v(\xi)$

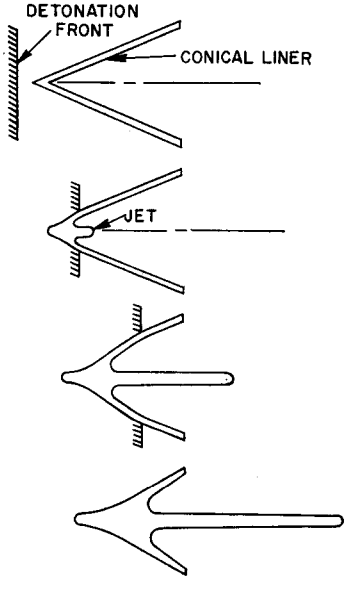


FIG. 1. Development of a shaped charge jet from a collapsing conical shell.

* Sponsored in part by Jet Research Center, Inc., Arlington, Texas.
† Head, Explosives Engineering Section, Poulter Laboratories, Stanford Research Institute.
‡ Professor of Engineering Mechanics, Stanford University, and Consultant, Stanford Research Institute.
[1] G. Birkhoff, D. P. MacDougall, E. M. Pugh, and G. I. Taylor, J. Appl. Phys. **19**, 563 (1948).
[2] D. C. Pack and W. M. Evans, Proc. Phys. Soc. (London) **64**, 298 (1951).
[3] R. J. Eichelberger, J. Appl. Phys. **27**, 63 (1956).
[4] S. Singh, Proc. Phys. Soc. (London) **70**, 867 (1957).
[5] M. A. Cook, J. Appl. Phys. **30**, 725 (1959).
[6] W. A. Allen, G. E. Meloy, and J. W. Rogers, "Hypervelocity Precision Impact Instrument," *Proceedings of the Hypervelocity Techniques Symposium* (Institute of Aeronautical Sciences, New York, 1960), p. 49.
[7] These effects are discussed elsewhere; see references 1–5.

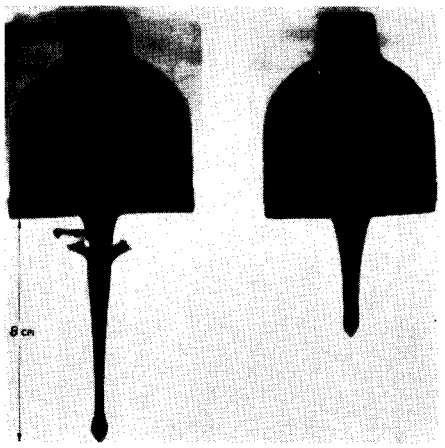


FIG. 2. Double flash x-ray photograph of a jet emerging from a shaped charge. The interval between the flashes was about 7 $\mu$sec.

of the element is unchanged until impact, the displacement of the element at time $t$ is

$$tv(\xi)=\xi(t)+P(t), \tag{1}$$

where $P(t)$ is penetration. If the penetration rate is $U(t)$, the velocity of an element of the jet with respect to the plane of impact (bottom of the hole) is $v(\xi)-U(t)$, as indicated in Fig. 5(b). The pressure at the stagnation point in Fig. 5(b) is the same for the jet and target. Hence, assuming steady flow conditions, Bernoulli's law gives

$$\rho(v-U)^2=\rho_1 U^2, \tag{2}$$

where $\rho$ is the density of the jet and $\rho_1$ is the density of the target. Since $v-U$ and $U$ are positive (2) gives

$$v=U[1+(\rho/\rho_1)^{\frac{1}{2}}]. \tag{3}$$

Differentiating (1) with respect to time, with $dP/dt=U$, and combining the resulting equation with (3) to eliminate $U$, we obtain

$$dt/d\xi+\alpha(v'/v)t=\alpha/v, \tag{4}$$

where $v'=dv/d\xi$ and $\alpha=1+(\rho/\rho_1)^{\frac{1}{2}}$. Regarding $v$ as a known function of $\xi$ and using $v^\alpha$ as an integrating factor, (4) gives

$$[v^\alpha t]_{\xi=S+l}-[v^\alpha t]_{\xi=S}=\alpha\int_S^{S+l} v^{\alpha-1}(\xi)d\xi. \tag{5}$$

Putting $[v]_{\xi=S}=v_0$, $[v]_{\xi=S+l}=v_1$, and noting that

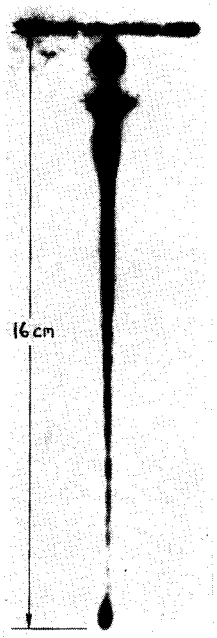


FIG. 4. Flash x-ray photograph illustrating jet break-up.

$[t]_{\xi=S}=S/v_0$, (5) may be combined with (1) to give

$$P=\left[(\beta+1/v_1{}^\beta)\int_S^{S+l} v^\beta d\xi-l\right]+S[(v_0/v_1)^\beta-1], \tag{6}$$

where $P$ is total penetration and $\beta=\alpha-1=(\rho/\rho_1)^{\frac{1}{2}}$. To show the effect of jet velocity distribution it is convenient to substitute $\eta=(\xi-S)/l$ in (6), with $0\leq\eta\leq1$ corresponding to $S\leq\xi\leq S+l$. Thus we obtain

$$P=l\left[(\beta+1/v_1{}^\beta)\int_0^1 v^\beta(\eta)d\eta-1\right]+S[(v_0/v_1)^\beta-1]. \tag{7}$$

For a jet of uniform velocity $v(\eta)=v_0=v_1$, and (7) reduces to

$$P=l(\rho/\rho_1)^{\frac{1}{2}}, \tag{8}$$

which is the result obtained earlier.[1,2]

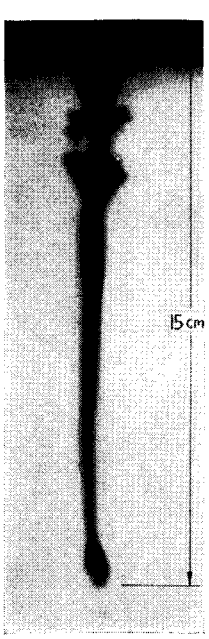


(a)

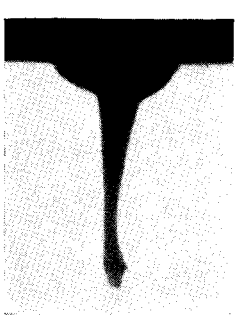

(b)

FIG. 3. Double flash x-ray photograph showing jet waver. The interval between flashes was about 15 $\mu$sec.

## III. DISCUSSION

The effect of jet velocity distribution on penetration is readily seen from (7). For fixed $v_1$, $v_0$, and $S$, penetration is maximized by giving $v(\eta)$ the greatest possible values for $0<\eta<1$. With the restriction $dv/d\eta \leq 0$, this is accomplished by giving the entire jet, except the element at the rear, the velocity $v_0$. Then (7) yields

$$P_i = l[(\beta+1)(v_0/v_1)^\beta - 1] + S[(v_0/v_1)^\beta - 1], \quad (9)$$

where $P_i$ denotes "ideal" penetration. The penetration given by (9) can never be realized in practice because it is for a jet with the velocity gradient concentrated at the rear; thus the rear of the jet is of infinitesimal thickness. Nevertheless, the ideal penetration is useful as an upper bound.

The effect of stand-off on penetration is evident in (7). For a jet of uniform velocity penetration is independent of stand-off, and (7) (with $v_0=v_1$) conforms to this. For $v_0>v_1$, penetration increases with stand-off at a rate depending upon $\beta$. As mentioned above, the increase of actual penetration with stand-off is limited by jet break-up and waver.

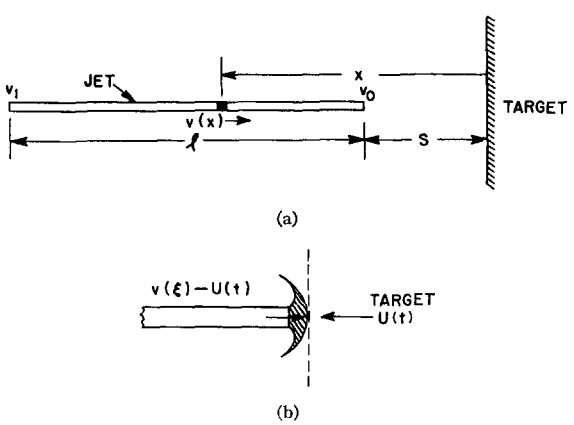


FIG. 5. Notation: (a) configuration at $t=0$, target stationary; (b) configuration at time $t$, bottom of hole stationary.

## IV. PENETRATION CALCULATION FOR A TYPICAL SHAPED CHARGE

As an illustrative example the foregoing theory may be used to calculate the penetration of the charge of Fig. 6, the velocity distribution for which is given by Eichelberger.[3] Figure 7 shows the velocity distribution as a function of axial distance from the top of the cone. The upper ends of the curves correspond to the front of the jet and the lower ends to the rear. The curve for $t=0$ is given by Eichelberger[3] as the basic description of the jet velocity distribution; from it the velocity distribution at any later time can be found. The curves for $t=0$ and $t=10.2$ are artificial since the point corresponding to the front of the jet is plotted to the left of $z=0$ (the top of the cone). They represent extrapolations of the experimental velocity distributions to times prior to the beginning of jet formation. This procedure is valid as long as the jet is allowed to form before it arrives at the target.

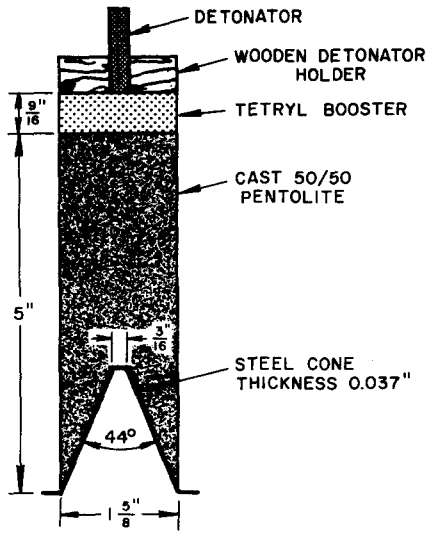


FIG. 6. Carnegie Institute of Technology (CIT) standard shaped charge; see reference 3.

The jet starts to form between $z=10.2$ $\mu$sec and 20.4 $\mu$sec, since the point representing the front of the jet in Fig. 7 passes the top of the cone in this interval. The straight line divides the jet approximately into formed and unformed parts It may be imagined that as a section of the velocity curve passes the line, the corresponding element of the jet forms. The entire jet is formed by $t=40.7$ $\mu$sec, at which time the front of the jet is 20 cm from the original location of the top of the cone.

The charge of Fig. 6 performs well at a stand-off distance of 10 cm. At this stand-off the velocity curve at the instant of impact with the target would lie between the curves for $t=30.5$ and $t=40.7$ $\mu$sec. Thus part of the jet is unformed when the front starts penetrating the target.

As indicated in Fig. 7, $\eta$ varies from zero at the front of the jet to unity at the rear. When the velocity distri-

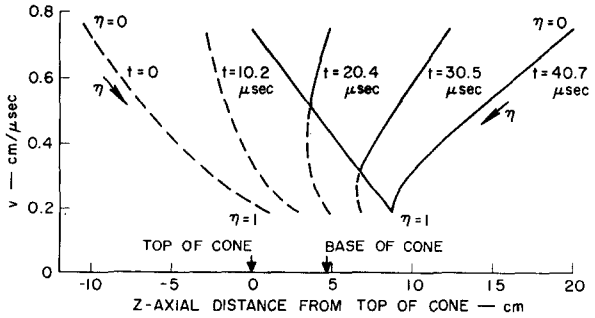


FIG. 7. Velocity distribution for the CIT standard charge. The dashed curves represent jet elements before formation, and the solid curves represent jet elements after formation.

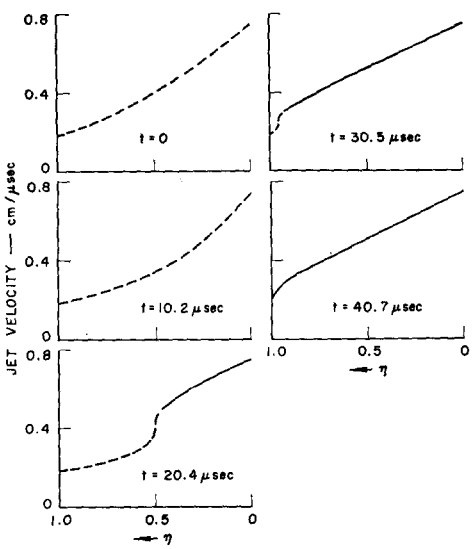


FIG. 8. Velocity distribution for the CIT standard charge as a function of $\eta$.

bution is plotted as a function of $\eta$, the curves of Fig. 8 are obtained. For $t=0$ and $t=10.2$ $\mu$sec, $v(\eta)$ is similar in shape to $v(z)$. However, for $t=20.4$, $v(\eta)$ has a sharp break due to the vertical tangent in $v(z)$. The same form is found for $t=30.5$ $\mu$sec. Subsequently, the velocity distribution becomes smooth again as shown by the curve for $t=40.7$ $\mu$sec.

The velocity curve for $t=20.4$ $\mu$sec in Fig. 7 shows the front of the jet at the base of the cone. It is convenient to use this particular velocity distribution in calculating penetration since the conventional interpretation of stand-off distance can then be retained. From (7), with $\beta=1$, $v_1=0.19$ cm/$\mu$sec, $v_0=0.75$ cm/$\mu$sec, $l=2.8$ cm,[8] and $\int_0^1 v(\eta)d\eta=0.44$, we find

$$P=10.2+3S. \tag{10}$$

For $S=10$ cm, (10) gives $P=40.2$ cm. This is substantially greater than the penetration of 12 cm reported[3] for the CIT charge. The discrepancy is attributed to jet and target strength effects, jet breakup, and waver. If only the part of the jet with velocity greater than 0.4 cm/$\mu$sec is used in the calculation, the penetration from (7) is

$$P=3.0+0.88S. \tag{11}$$

For $S=10$ cm, (11) yields $P=12$ cm, the same as the observed value. But since the other part of the jet, with velocity less than 0.4 cm/$\mu$sec, produces some penetration, the 12-cm penetration calculated for the forward part of the jet must be regarded as somewhat high. The apparent lower penetration obtained experimentally for the forward part of the jet is attributed[3] to jet break-up and waver.

[8] The velocity curve shows two velocities for a given axial coordinate. The extrapolated fictitious jet is folded over and is like a string in the shape of a flattened C, which is in process of straightening out. The length $l$ is the complete length, given by the sum of the horizontal spans of the upper and lower parts of the curve in Fig. 7.

## V. VARIATION IN JET VELOCITY DISTRIBUTION WITH TIME

For jets of nonuniform velocity the velocity distribution varies as the jet travels toward the target. It is readily shown that the variations always tend to produce a jet with a uniform velocity gradient. Let $x$ denote the distance from the front of the jet to a typical element and let $l$ be the length of the jet. At a time $t$ later the distance from the front to the element originally at $x$ is

$$x'=x+[v_0-v(x)]t \tag{12}$$

and the new length of the jet is

$$l'=l+(v_0-v_1)t. \tag{13}$$

Dividing (12) by (13), putting $\eta=x/l$, and $\eta'=x'/l'$, yields

$$\eta'=\frac{\eta+[v_0-v(\eta)]t/l}{1+(v_0-v_1)t/l}. \tag{14}$$

The velocity gradient may be written

$$\frac{dv}{d\eta'}=\frac{dv}{d\eta}\frac{d\eta}{d\eta'}. \tag{15}$$

With $d\eta/d\eta'$ from (14), (15) becomes

$$\frac{dv}{d\eta'}=\frac{dv}{d\eta}\left[\frac{1+(v_0-v_1)t/l}{1-(dv/d\eta)(t/l)}\right]. \tag{16}$$

As $t$ increases indefinitely, (16) gives

$$\frac{dv}{d\eta'}=-(v_0-v_1). \tag{17}$$

Thus the velocity distribution becomes linear at sufficiently large $t$.

The change in velocity gradient for smaller values of $t$ may be seen by comparing the coefficient of $t/l$ in the numerator and denominator of the bracketed factor in (16). The coefficient of $t/l$ in the numerator is the average velocity gradient. That in the denominator is the negative of the velocity gradient at $\eta$ and is always positive if we take $dv/d\eta<0$. Hence the bracketed factor is greater than unity for $|dv/d\eta|<(v_0-v_1)$ and is less than unity for $|dv/d\eta|>(v_0-v_1)$. Thus the velocity distribution is always changing towards the linear form. This is consistent with the observation[1] that shaped charge jets generally have nearly linear velocity distributions. The velocity curves of Figs. 7 and 8 illustrate this effect. (Only the portion of the jet which has formed should be considered.)

## VI. PENETRATION OF A JET WITH A LINEAR VELOCITY DISTRIBUTION

We now compare the ideal penetration of (9) with the penetration for a jet with an initial linear velocity distribution. With the linear velocity distribution

$$v(\eta)=v_0\{1+\eta[(v_1/v_0)-1]\} \tag{18}$$

and $\beta=1$, (7) gives

$$P=l(v_0/v_1)+S[(v_0/v_1)-1]. \tag{19}$$

The ideal penetration from (9), with $\beta=1$, is

$$P_i=l[(2v_0/v_1)-1]+S[(v_0/v_1)-1]. \tag{20}$$

For $v_0/v_1=3$, a reasonable choice, the ratio of the penetrations from (19) and (20) is

$$P/P_i=(3l+2S)/(5l+2S). \tag{21}$$

For the charge used in the example above the stand-off distance (10 cm) is about four times the length of the jet (2.8 cm) at $t=20.4$ $\mu$sec (see Fig. 7). If $S=4l$, (18) gives $P/P_i=0.85$. Thus a jet with a linear initial velocity distribution gives about 85% of the ideal penetration. This indicates that there is little to be gained by modifying jet velocity distributions beyond the linear form. A more profitable approach would be to increase $v_0/v_1$. Since the lower limit on $v_1$ is fixed by the strength of the jet and target, this must be accomplished by increasing $v_0$.

## VII. EFFECT OF PROJECTILE VELOCITY

The effect of increasing the average velocity of a jet, perhaps by launching the charge with a rocket, is readily seen from (7). Adding a uniform velocity to $v(\eta)$ increases the value of the integral in (7). However, the denominator $v_1{}^\beta$ shows a greater proportional increase, since $v_1$ is the least value of $v(\eta)$. Hence the factor multiplying $l$ actually decreases. The same is true for the factor multiplying $S$. Thus, for a jet and target which satisfy the assumptions of the theory, the addition of a uniform velocity would cause a decrease in penetration.

If, however, a portion of the rear of the jet has a velocity which is less than that required to overcome the strength of the jet and target, $v_1$ in (7) would remain constant with addition of a uniform velocity (until all of the jet is traveling at a velocity sufficient to overcome jet and target strength) and $v_0$ would increase. Thus, up to a limit, penetration would increase with addition of a uniform velocity.

All these conclusions of course concern an idealized jet free from break-up and waver, effects which are important in determining the performance of real jets.

## ACKNOWLEDGMENTS

The authors are grateful for the assistance of the late J. E. Neimark and M. Weisfeld.